

Equilibrium Isotherms and Kinetics Modelling for an Efficient Removal of 4-Chloro-2-Methoxyphenol From Aqueous Solution Using Optimal Activated Carbon



Zaharaddeen N. Garba^{1*}, I. Ibrahim¹, Afidah Abdul Rahim²

¹Department of Chemistry, Ahmadu Bello University, Zaria, Nigeria

²School of Chemical Sciences, Universiti Sains Malaysia, Penang, Malaysia

*Correspondence to

Zaharaddeen N. Garba,
Tel.: +2348039443335,
Email: dinigetso2000@gmail.com

Published online June 29, 2021



Abstract

A surface area of 1085.92 m²/g and a monolayer adsorption capacity of 497.66 mg/g were obtained from the optimum activated carbon derived using *Prosopis africana* seed hulls (PASH-AC) at the activation temperature of 795°C, activation time of 62 minutes, and impregnation ratio of 2.45. Five different forms of the linearized Langmuir equations along with two other models (Freundlich and Temkin) were tested on the adsorption data. The best adsorption model was selected using correlation coefficient (R²) and chi-square (χ²) was used for assessing the validity of each isotherm model. Langmuir-2 along and pseudo-second-order models were found to be the most suitable model for describing the equilibrium and kinetic processes, respectively.

Keywords: *Prosopis africana* seed hulls, Activated carbon, Isotherms and kinetics modelling, Adsorption, 4-Chloro-2-methoxy phenol

Received May 8, 2021; Revised June 10, 2021; Accepted June 20, 2021

1. Introduction

In recent times, the pollution of water is among the main challenges of the environment distressing the modern world (1-7). Organic-based chemical contaminants such as chlorophenols are among water pollutants. Pharmacological similarities exist between chemical contaminants such as guaiacols and phenol. Chlorinated forms of guaiacols are quite similar to chlorophenols. They pose severe health hazards by affecting human nervous as well as respiratory systems. They have a strong odor, are not readily biodegradable, and are persistent in the environment. Additionally, they are toxic and have carcinogenic features (8,9)

One of the most valuable and effective control technologies for wastewater treatment is adsorption (10-17). Activated carbon (AC) is the best practical adsorbent due to its easy operation as well as good adsorption capacity (18-21). ACs are considered adsorbents as a result of their adaptable exterior properties which are broadly applied for a wide range of industries (12,19,22-24). The transformation of unwanted material from agriculture into valuable products towards the elimination of a possible pollutant in a cost-effective and eco-friendly manner has been suggested as an ingenious technique. Our previous studies have described the optimal conditions for AC preparations using *Prosopis africana*

seed hulls (PASH) (25-27) but no report on the removal of 4-chloro-2-methoxy phenol (4C2MP) from synthetic wastewater using CH₃COONa impregnated PASH-AC was found in the literature.

This work is therefore aimed at investigating the influence of the initial concentration of 4C2MP, time of adsorption, and solution pH on the PASH-AC with sodium acetate (CH₃COONa) utilized as the activating chemical agent to remove 4C2MP. Other investigations carried out on the PASH-AC are based on equilibrium data modelling, kinetics, and thermodynamics study.

2. Materials and Methods

2.1. Preparation and Characterization of Adsorbent (PASH-AC)

The precursor (PASH) used in this study was prepared in Zaria, Nigeria, using a similar optimization technique applied in our earlier work (25). The AC was prepared using sodium acetate as an activating agent, and the dried precursor (of the desired particle size) was measured and mixed with the activating agent at different ratios. The mixture was heated in a water bath (80–90°C) overnight and dried in an oven for 24 hours to remove moisture before loading into a furnace embedded in a tubular reactor. The carbonization step involved heating the reactor at 700°C under purified nitrogen (99.99%)

atmosphere with the flow rate of 150 mL/min. The carbonized material was then activated under CO₂ gas at a flow rate of 150 mL/min using a reactor similar to the one used for carbonization under different temperatures and held for varying periods of time. The product was cooled to room temperature, washed with distilled water until a neutral pH was attained, oven dried, and finally stored in an airtight container for further use. Similar optimal preparation conditions (activation temperature of 795°C, activation time of 62 minutes, and impregnation ratio of 2.45) as reported in our earlier work were applied (25) which produced PASH-AC with reasonable yield, thereby removing a significant amount of 4C2MP.

Scanning electron microscopy (SEM) analysis was carried out on the AC prepared at the optimum conditions using FEI QUANTA PEG 60 model to study its surface morphology with the surface functional groups of the adsorbent detected using FTIR spectroscopy (FTIR-2000, Perkin Elmer, GX infrared spectroscopy) and spectra were recorded at 4000-400 cm⁻¹ range.

The pH point of zero charge (pH_{pzc}) was determined by adopting solid addition method similar to the method which involved the addition of adsorbent sample (0.1 g) into 100 mL conical flasks containing

50 mL of various concentrations of KNO₃ (0.1, 0.01, 0.001 mol dm⁻³). To adjust the initial pH of the KNO₃ solution from 2 to 12, 0.1 M KOH and HCl were used. The sample was shaken at 180 rpm until equilibrium was established, and the final pH was recorded. The final pH was plotted against initial pH values of the solution with plateau point on the plot noted and recorded as the pH_{pzc} of the adsorbent.

2.2. Batch Adsorption of 4C2MP

Experiments were carried out using batch adsorption to remove 4C2MP by PASH-AC as reported previously (25).

At equilibrium (% R), the percentage of 4C2MP removed was estimated as:

$$4C2MP \text{ removal (\%)} = \frac{C_o - C_e}{C_o} \times 100 \quad (1)$$

where C_o and C_e (mg/L) represent the initial and equilibrium concentrations, respectively.

The equilibrium amount of 4C2MP adsorbed, q_e (mg/g), was evaluated by equation 2:

$$q_e = \frac{(C_o - C_e)V}{W} \quad (2)$$

The kinetics of adsorption process was analysed by estimating 4C2MP concentration at different times. The degree of 4C2MP adsorbed at time t, q_t (mg/g), was estimated by equation 3:

$$q_t = \frac{(C_o - C_t)V}{W} \quad (3)$$

Solutions pH as well as functional group were determined using the same process as reported in our earlier published work (11).

3. Results and Discussion

3.1. Characterization of PASH-AC

Figs. 1a and 1b show the SEM images of the raw PASH and the PASH-AC, respectively.

The surface texture of the precursor was rough, uneven, undulating, and porous. As shown in Fig. 1b, homogeneous porous structures were distributed on the surface of the PASH-AC. This result revealed that the combined activation process of CH₃COONa and CO₂ was effective in creating well-developed pores, resulting in AC with a large surface area and a good mesoporous structure. Other researchers have described similar observations on coconut husk (28), *Borassus aethiopicum* shells (29), oil

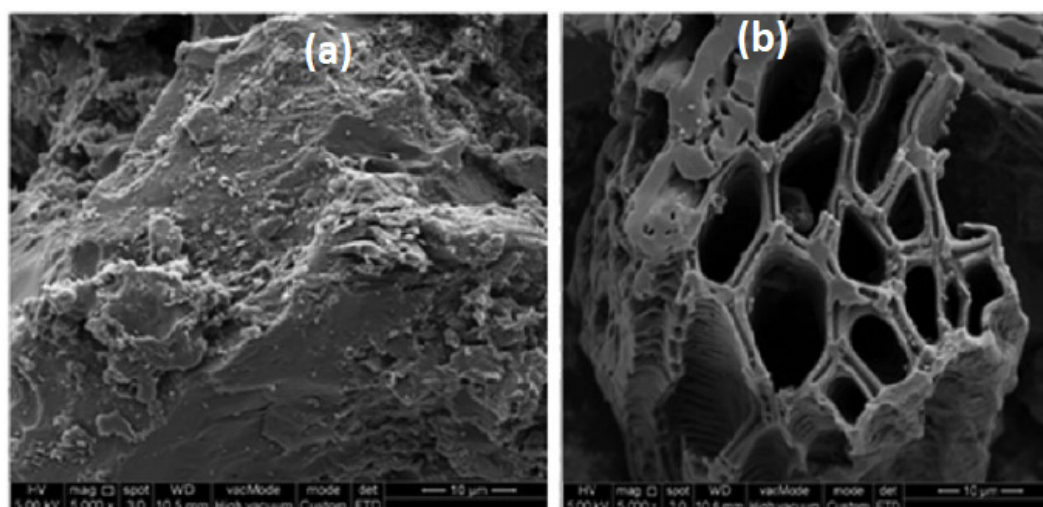


Fig. 1. SEM Micrograph of (a) Raw PASH Sample and (b) PASH-Based Activated Carbon.

palm shell (30), and *Canarium schweinfurthii* seed shell (12).

A disparity can be observed upon comparing the PASH and PASH-AC spectra (Fig. 2).

The broad bands observed at 3500-3200 cm⁻¹, 3300-3000 cm⁻¹ and 3000-2800 cm⁻¹ correspond to O-H, N-H and both saturated as well as unsaturated C-H groups, respectively. The feeble peak observed around 700-800 cm⁻¹ was assigned to C-OH (out of plane bending) in phenol. Carbonization followed by activation was responsible for the disappearance of several functional groups as observed in the PASH-AC spectra. This observation was ascribed to the effect of thermal degradation, which led to the obliteration of intermolecular bonding.

The pH_{pzc} of the adsorbent was found to be 6.53, revealing that the surface area of the adsorbent was larger on the acidic group. A similar observation was reported by other researchers (31).

3.2. Impact of the Concentration of 4C2MP and the Time of Adsorption

A fast increase in 4C2MP concentrations can be observed in Fig. 3a, followed by a slow uptake until equilibrium, which was attained at minimum time for lower initial concentrations. The variance in equilibrium time realization was ascribed to the quicker elimination or vanishing of adsorbate molecules at dissimilar adsorbate concentrations (31)

3.3 Influence of Solution pH

As depicted in Fig. 3b, the percentage of 4C2MP removal indicated a substantial decline with a rise in the pH of the solution from 2 to 12. At pH 2. A removal percentage of 95.81% was attained, which was attributed to its great affinity to form hydrogen bonding with the external surface of the PASH-AC as a result of the methoxy group asserting the influence of withdrawing group (32).

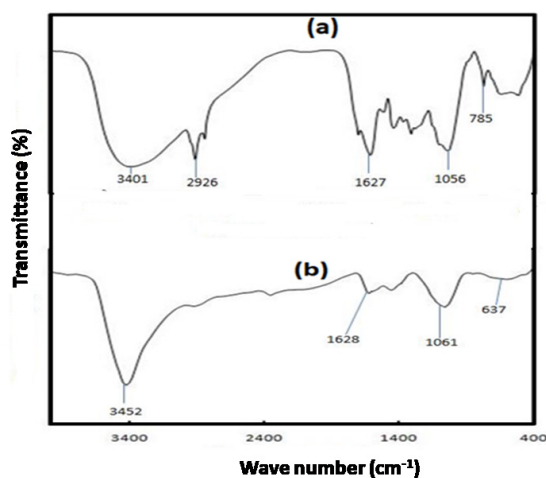


Fig. 2. FT-IR Spectra of (a) PASH and (b) PASH-AC.

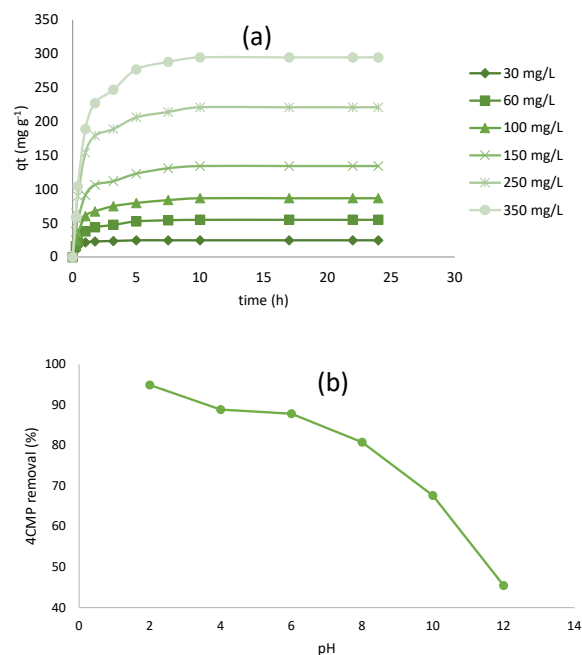


Fig. 3. (a) Effect of Contact Time on 4C2MP Adsorption Onto PASH-AC at Various Initial Concentrations (b) Effect of Solution pH on 4C2MP Removal by PASH-AC .

3.4. Adsorption Isotherms Modelling

Langmuir (L1-L5), Freundlich (F), and Temkin (T) isotherm models were used to investigate the equilibrium data.

Langmuir isotherm is widely used for the elimination of water pollutants, described by equation 4 (33):

$$q_c = \frac{K_L Q_a^0 C_c}{1 + K_L C_c} \tag{4}$$

The constants of the isotherm linked to the adsorption capacity and rate were represented as Q_a^0 (mg/g) and K_L (L/mg), respectively. Equation 4 was conveyed in five dissimilar linear forms, as presented in Table 1, with great discrepancies associated with the dispersal of the data and the accuracy of parameter determination (34).

Another important adsorption parameter called dimensionless separation factor (R_L) is defined as (35):

$$R_L = \frac{1}{1 + K_L C_o} \tag{5}$$

where C_o denotes the concentration of 4C2MP. R_L values indicate whether the adsorption is unfavourable ($R_L > 1$), linear ($R_L = 1$), favourable ($0 < R_L < 1$), or irreversible ($R_L = 0$).

The adsorption process on a surface that is heterogeneous is described by Freundlich (F) isotherm which is described as (36):

$$\log q_c = \log K_F + \frac{1}{n} \log C_c \tag{6}$$

where K_F and n stand for adsorption capacity deviation of the model from linearity, respectively. Generally, the higher the n value, the more favourable the adsorption process.

The third model applied to the generated adsorption data was Temkin (T) model, depicted as (37):

$$q_e = \frac{RT}{b} \ln A + \frac{RT}{b} \ln C_e \quad (7)$$

For the proper understanding of the model legitimacy in explaining the process, χ^2 was calculated and considered due to uncertainty about the use of correlation coefficient (R^2) only as it is no longer reliable in selecting the most suitable model since it only explains the correlation between linear forms of the isotherm equations and experimental data with χ^2 best describing the appropriateness between predicted and experimental values of the adsorption capacity. Better fit is indicated by the lower χ^2 value.

As can be observed in Table 2, there are varying values deducted from the five linear L equations, because the original error distribution was altered by the transformations (34).

Table 1. Linear Forms of Langmuir Isotherm

Isotherm	Linear Form	Plot
L-1	$\frac{1}{q_e} = \frac{1}{K_L Q_a^0 C_e} + \frac{1}{Q_a^0}$	$\frac{1}{q_e}$ vs $\frac{1}{C_e}$
L-2	$\frac{C_e}{q_e} = \frac{C_e}{Q_a^0} + \frac{1}{K_L Q_a^0}$	$\frac{C_e}{q_e}$ vs C_e
L-3	$q_e = -\frac{q_e}{K_L C_e} + Q_a^0$	q_e vs $\frac{q_e}{C_e}$
L-4	$\frac{q_e}{C_e} = -K_L q_e + K_L Q_a^0$	$\frac{q_e}{C_e}$ vs q_e
L-5	$\frac{1}{C_e} = \frac{K_L Q_a^0}{q_e} - K_L$	$\frac{1}{C_e}$ vs $\frac{1}{q_e}$

Table 2. Langmuir (L-1 to L-5), Freundlich (F), and Temkin (T) Isotherm Model Parameters (Correlation Coefficients and Chi-square Values) for 4C2MP Adsorption on PASH-AC at 30°C

Langmuir	Isotherm Parameters			
	Q_a^0 (mg/g)	RL	R^2	χ^2
L-1	334.21	0.045	0.9920	4.380
L-2	497.66	0.074	0.9665	0.393
L-3	449.48	0.064	0.8625	2.475
L-4	498.54	0.073	0.8625	9.740
L-5	343.56	0.046	0.9920	5.725
F	K_F (mg/g (L/mg))	n	R^2	χ^2
	22.30	1.382	0.9876	1.420
T	A (L/g)	B (J/mol)	R^2	χ^2
	0.620	84.385	0.9281	31.750

L-1 or L-5 was determined to be the most suitable isotherm to describe the adsorption process based on the R^2 values obtained since they exhibited the largest values ($R^2 = 0.9920$). However, higher R^2 values are no longer reliable in describing the best transformations according to (34). As can clearly be seen in Table 2, the highest R^2 values ($R^2 = 0.9920$) were exhibited by L-1 and L-5, however, the χ^2 values shown by those models were high, larger than 0.393 obtained from L-2. Therefore, L-1 and L-5 cannot be reliable in perfectly describing the equilibrium data. Another important observation from Table 2 is that the χ^2 values obtained from F (1.420) as well as T (31.750) were also greater than 0.393 obtained from the L-2 isotherm, indicating that it was the most reliable model in describing the adsorption process. Therefore, 497.67 mg/g and 0.074 were selected as the correct values for the maximum adsorption capacity (Q_a^0 and separation factor (R_L), respectively, which were picked up from the L-2 equation.

The high Q_a^0 value (497.67 mg/g) adopted in this work was ascribed to the mesoporous nature as well as the large surface area of PASH-AC (25). It performed very well upon comparison with values compiled from previous researchers in Table 3.

3.5. Adsorption Kinetic Studies

Lagergren pseudo-first-order and pseudo-second-order (1 and 2) were the popular kinetic models applied in studying the 4C2MP adsorption process. The linear equation of pseudo-first-order was given as (41):

$$\log(q_e - q_t) = \log q_e - \frac{k_1}{2.303} t \quad (8)$$

The pseudo-second-order equations were depicted in two forms as in equations 9 and 10:

$$\frac{t}{q_t} = \frac{1}{k_2 q_c^2} + \frac{1}{q_c} t \quad (9)$$

$$\frac{1}{q_t} = \left(\frac{1}{k_2 q_c^2} \right) \frac{1}{t} + \frac{1}{q_c} \quad (10)$$

All the values obtained from the linear plots of equation 8 (Fig. 4a) as well as equations 9 and 10 (Fig. 4b and 4c) for the 4C2MP adsorption process were tabulated (Table 4). There was no coherence in the trends shown by the R^2 values obtained from the pseudo-first-order model (0.741-0.952). In addition, there was a poor correlation between the calculated as well as the experimental q_c values, indicating the unsuitability of the model for properly explaining the process of 4C2MP adsorption onto PASH-AC. However, similarity was observed when the q_c values (calculated and experimental) deducted from pseudo-second-order models were compared with each other, indicating that almost all the obtained R^2 values were very close to one, thereby re-affirming the suitability

Table 3. Comparison of Maximum Monolayer Adsorption Capacity of Various Chlorophenols on Different Adsorbents

Adsorbent	Adsorbate	Q _s ⁰ (mg/g)	Reference
PASH-AC	4-Chloro2-methoxy phenol	497.66	This work
Commercial activated carbon	4-Chloro2-methoxy phenol	276.88	This study
Oil palm shell activated carbon	4-Chloro2-methoxy phenol	323.62	(32)
Oil palm shell activated carbon	4-Chloroguaiacol	454.45	(30)
Rattan sawdust based activated carbon	4-chlorophenol	188.68	(38)
Cattail fiber-based activated carbon	2,4-Dichlorophenol	142.86	(39)
Rice straw carbon	3-chlorophenol	14.2	(40)

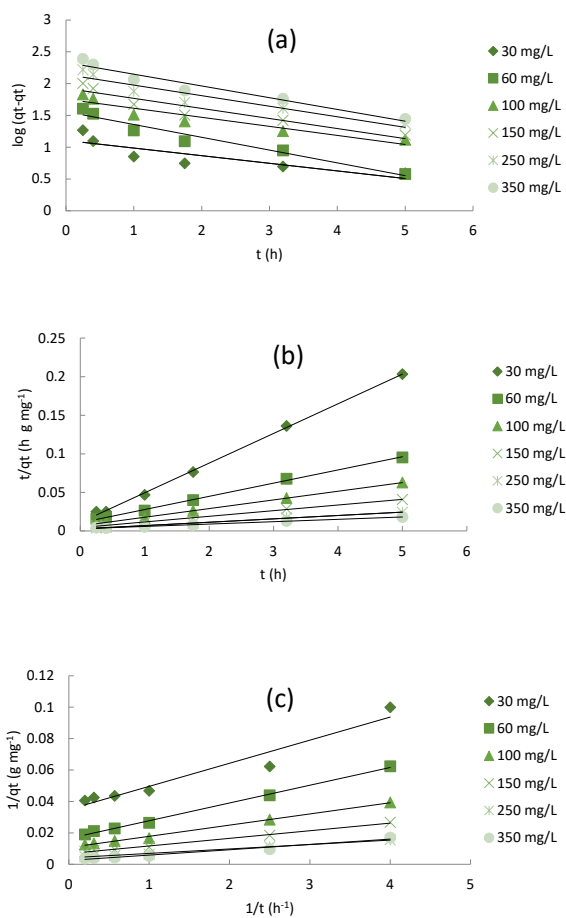


Fig. 4. Linearized Plots of (a) Pseudo-First-Order (b) Pseudo-Second-Order 1 and (c) Pseudo Second-Order 2 Kinetic Models for 4C2MP Adsorption on PASH-AC at 30°C .

of pseudo-second-order model as the most reliable kinetic model in describing the adsorption process of 4C2MP onto PASH-AC. Furthermore, the lower the χ^2 values (0.001-1.999) obtained from both the pseudo-second-order 1 and 2 models upon comparison with those acquired from the pseudo-first-order (11.164-59.109) further confirmed the suitability of pseudo-second-order equation as the best kinetic model to describe the 4C2MP adsorption onto PASH-AC. The failure of kinetic models

in the description as well as proper detection of diffusion mechanisms prompted intraparticle diffusion model to be applied, which was mathematically described as:

$$q_t = k_{ip} t^{1/2} + C \tag{11}$$

As shown in Fig. 5, there was very rapid adsorption at the beginning attributed to the electrostatic attraction which was strong between 4C2MP and the external surface of PASH-AC.

That was followed by a stage of steady adsorption, ascribed to intraparticle diffusion of the 4C2MP molecule through the adsorbent. In some cases, when the intraparticle diffusion begins to slow down, a third stage exists. The start stage is usually possible when the initial concentration of the adsorbate is high (42).

An increase in the k_{p2} values can be noticed in Table 5 which keeps rising with an increase in the initial concentration of 4C2MP. That was attributed to a strong driving force. Furthermore, there was an upsurge in the values of C_2 and C_3 with the increase in 4C2MP concentration from 30 to 350 mg/L, suggesting the boundary layer to be thicker (43). It can also be observed from Fig. 5 with respect to the second and third stages that the linear lines evaded the origin .

3.6. Thermodynamic Studies of Adsorption

The three most popular thermodynamic parameters

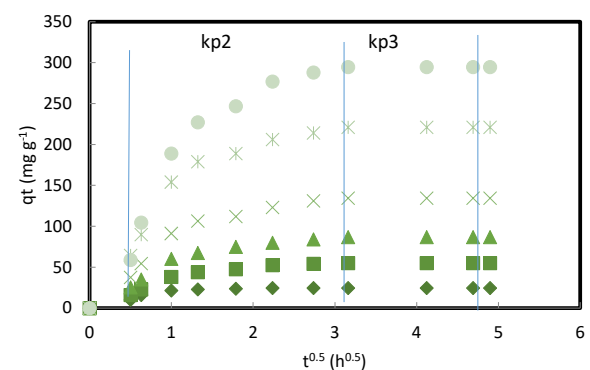


Fig. 5. Plot of Intraparticle Diffusion Model for Adsorption of 4C2MP onto PASH-AC at 30°C .

Table 4. Pseudo-First-Order and Pseudo-Second-Order (1 & 2) Kinetic Model Parameters of 4C2MP Adsorption on PASH-AC at 30°C

C_o (mg/L)	$q_{e,exp}$ (mg/g)	Pseudo-First-Order			Pseudo-Second-Order-1			Pseudo-Second-Order-2					
		k_1 (1/h)	$q_{e,cal}$ (mg/g)	R^2	k_2 (g/mg h)	$q_{e,cal}$ (mg/g)	R^2	χ^2	k_2 (g/mg h)	$q_{e,cal}$ (mg/g)	R^2	χ^2	
30	28.51	0.276	12.78	0.741	19.361	0.134	26.04	0.999	0.234	0.083	28.65	0.943	0.001
60	56.29	0.463	36.19	0.952	11.164	0.028	58.48	0.998	0.082	0.024	60.98	0.997	0.361
100	92.83	0.328	56.95	0.889	22.605	0.019	89.29	0.999	0.140	0.016	93.46	0.996	0.004
150	138.47	0.366	84.47	0.895	34.521	0.012	136.99	0.998	0.016	0.094	147.06	0.994	0.502
250	229.63	0.383	138.99	0.898	59.109	0.008	227.27	0.998	0.025	0.006	243.90	0.996	0.835
350	304.75	0.426	215.38	0.942	37.083	0.003	322.58	0.993	0.986	0.002	330.45	0.974	1.999

Table 5. Intraparticle Diffusion Model Parameters for the Adsorption of 4C2MP onto PASH-AC

C _o (mg/L)	Intraparticle Diffusion Model					
	k _{p2} (mg/g h ^{1/2})	k _{p3} (mg/g h ^{1/2})	C ₂	C ₃	(R ₂) ²	(R ₃) ²
30	7.142	-	10.852	24.610	0.7280	-
60	20.072	0.2227	11.723	53.843	0.8828	0.4919
100	30.457	0.9199	19.147	82.518	0.8662	0.4919
150	46.831	1.1000	29.012	129.240	0.8563	-
250	78.519	2.3075	49.089	210.510	0.8554	-
350	118.80	2.2432	55.698	284.450	0.8819	-

namely, change in Gibb's free energy (ΔG), change in enthalpy (ΔH), and the change in entropy (ΔS) were evaluated using van 't Hoff equation, mathematically expressed as (44):

$$\ln K_D = \frac{\Delta S}{R} - \frac{\Delta H}{RT} \quad (12)$$

$K_D = \frac{q_e}{C_e}$ is the distribution coefficient; q_e (mg/g) is the amount of adsorbate adsorbed on the sorbent per unit mass. The values of ΔS and ΔH were obtained from the intercept and slope of a linear plot of $\ln K_D$ against $1/T$ (Figure not shown), and ΔG was evaluated using Eq. (13):

$$\Delta G = -RT \ln K_D \quad (13)$$

Endothermic 4C2MP adsorption process with disorderliness was predicted based on the positive values obtained for both ΔH and ΔS , respectively (Table 6).

Furthermore, the negative ΔG values obtained signified a spontaneous process, the higher the negative ΔG value, the more spontaneous the adsorption process. This phenomenon has also been observed in the adsorption of 2,4,6-TCP on activated clay (45). The ΔG values (-6.45 to -6.88) further confirm that the adsorption process of 4C2MP onto PASH-AC is a physical one with the physical adsorption values extending from -20 to 0 kJ/mol while values from -80 to -400 kJ/mol indicate chemical adsorption (46). This phenomenon was also observed in the adsorption of chlorophenols onto other adsorbents (39,47,48).

Conclusion

PASH-AC was successfully produced from *Prosopis africana* seed hulls with its adsorption capacity reported to be surging up with an increase in both initial concentration of 4C2MP as well as adsorption time. Acidic solution was

the most favourable route for the adsorption process with the suitability of Langmuir-2, which was reported as the best isotherm model for describing the equilibrium data. Pseudo-second-order model was the best kinetic model for describing the kinetic process of 4C2MP adsorption onto PASH-AC with the mechanism primarily guided by particle diffusion according to the Boyd plot. Endothermic process was also confirmed based on the positive ΔH values observed with its great potential upon comparison with previously reported results available in the literature. The obtained results may be a good base for claiming the effectiveness of PASH-AC produced in tackling pollution problems posed by contaminants belonging to chloroguaicols in the environment.

Conflict of Interest Disclosures

The authors declare that they have no conflict of interests.

References

- Galadima A, Garba ZN, Leke L, Almustapha MN, Adam IK. Domestic water pollution among local communities in Nigeria-causes and consequences. *Eur J Sci Res.* 2011;52(4):592-603.
- Sun S, Xiao W, You C, Zhou W, Garba ZN, Wang L, et al. Methods for preparing and enhancing photocatalytic activity of basic bismuth nitrate. *J Clean Prod.* 2021;294:126350. doi: 10.1016/j.jclepro.2021.126350.
- Sun S, Jiang X, Xiao W, Jiang Y, Zhou W, Lawan I, et al. A simple method for construction of Bi₂O₃/Bi₆O₆(OH)₃(NO₃)₃·1.5H₂O p-n junction photocatalyst with superior photocatalytic performance. *Mater Lett.* 2020;276:128199. doi: 10.1016/j.matlet.2020.128199.
- Surip SN, Abdulhameed AS, Garba ZN, Syed-Hassan SSA, Ismail K, Jawad AH. H₂SO₄-treated Malaysian low rank coal for methylene blue dye decolourization and cod reduction: optimization of adsorption and mechanism study. *Surf Interfaces.* 2020;21:100641. doi: 10.1016/j.surfin.2020.100641.
- Hui Chuin CT, Sabar S, Haafiz MK, Garba ZN, Hussin MH. The improved adsorbent properties of microcrystalline cellulose from oil palm fronds through immobilization technique. *Surf Interfaces.* 2020;20:100614. doi: 10.1016/j.surfin.2020.100614.
- Ahmad NL, Zakariyya UZ, Zaharaddeen NG. Rice husk as biosorbent for the adsorption of methylene blue. *Sci World J.* 2019;14(2):66-70.

Table 6. Thermodynamic Parameters for the Adsorption of 4C2MP onto PASH-AC at Different Temperatures

ΔH (kJ/mol)	ΔS (J/mol K)	ΔG (kJ/mol)		
		303 K	313 K	323 K
0.03	21.47	-6.45	-6.74	-6.88

7. Singh NB, Nagpal G, Agrawal S, Rachna. Water purification by using Adsorbents: a review. *Environ Technol Innov*. 2018;11:187-240. doi: [10.1016/j.eti.2018.05.006](https://doi.org/10.1016/j.eti.2018.05.006).
8. Armenante PM, Kafkewitz D, Lewandowski GA, Jou CJ. Anaerobic-aerobic treatment of halogenated phenolic compounds. *Water Res*. 1999;33(3):681-92. doi: [10.1016/S0043-1354\(98\)00255-3](https://doi.org/10.1016/S0043-1354(98)00255-3).
9. Tan IAW, Ahmad AL, Hameed BH. Adsorption isotherms, kinetics, thermodynamics and desorption studies of 2,4,6-trichlorophenol on oil palm empty fruit bunch-based activated carbon. *J Hazard Mater*. 2009;164(2-3):473-82. doi: [10.1016/j.jhazmat.2008.08.025](https://doi.org/10.1016/j.jhazmat.2008.08.025).
10. Adetokun AA, Uba S, Garba ZN. Optimization of adsorption of metal ions from a ternary aqueous solution with activated carbon from *Acacia senegal* (L.) Willd pods using Central Composite Design. *J King Saud Univ Sci*. 2019;31(4):1452-62. doi: [10.1016/j.jksus.2018.12.007](https://doi.org/10.1016/j.jksus.2018.12.007).
11. Abdul Rahim A, Garba ZN. Efficient adsorption of 4-chloroguaiacol from aqueous solution using optimal activated carbon: equilibrium isotherms and kinetics modeling. *J Assn Arab Univ Basic Appl Sci*. 2016;21:17-23. doi: [10.1016/j.jaubas.2015.09.001](https://doi.org/10.1016/j.jaubas.2015.09.001).
12. Garba ZN, Hussin MH, Galadima A, Lawan I. Potentials of *Canarium schweinfurthii* seed shell as a novel precursor for CH₃COOK activated carbon: statistical optimization, equilibrium and kinetic studies. *Appl Water Sci*. 2019;9(2):31. doi: [10.1007/s13201-019-0907-y](https://doi.org/10.1007/s13201-019-0907-y).
13. Garba ZN, Zhou W, Lawan I, Xiao W, Zhang M, Wang L, et al. An overview of chlorophenols as contaminants and their removal from wastewater by adsorption: a review. *J Environ Manage*. 2019;241:59-75. doi: [10.1016/j.jenvman.2019.04.004](https://doi.org/10.1016/j.jenvman.2019.04.004).
14. Hussin MH, Pohan NA, Garba ZN, Kassim MJ, Abdul Rahim A, Brosse N, et al. Physicochemical of microcrystalline cellulose from oil palm fronds as potential methylene blue adsorbents. *Int J Biol Macromol*. 2016;92:11-9. doi: [10.1016/j.ijbiomac.2016.06.094](https://doi.org/10.1016/j.ijbiomac.2016.06.094).
15. Xiao W, Garba ZN, Sun S, Lawan I, Wang L, Lin M, et al. Preparation and evaluation of an effective activated carbon from white sugar for the adsorption of rhodamine B dye. *J Clean Prod*. 2020;253:119989. doi: [10.1016/j.jclepro.2020.119989](https://doi.org/10.1016/j.jclepro.2020.119989).
16. Xiao W, Jiang X, Liu X, Zhou W, Garba ZN, Lawan I, et al. Adsorption of organic dyes from wastewater by metal-doped porous carbon materials. *J Clean Prod*. 2021;284:124773. doi: [10.1016/j.jclepro.2020.124773](https://doi.org/10.1016/j.jclepro.2020.124773).
17. Yang D, Zhao X, Zou X, Zhou Z, Jiang Z. Removing Cr(VI) in water via visible-light photocatalytic reduction over Cr-doped SrTiO₃ nanoplates. *Chemosphere*. 2019;215:586-95. doi: [10.1016/j.chemosphere.2018.10.068](https://doi.org/10.1016/j.chemosphere.2018.10.068).
18. Garba ZN, Abdullahi AK, Haruna A, Gana SA. Risk assessment and the adsorptive removal of some pesticides from synthetic wastewater: a review. *Beni Suef Univ J Basic Appl Sci*. 2021;10(1):19. doi: [10.1186/s43088-021-00109-8](https://doi.org/10.1186/s43088-021-00109-8).
19. Garba ZN, Abdul Rahim A. Adsorption of 4-chlorophenol onto optimum activated carbon from an agricultural waste. *Int J Sci Res*. 2015;4(5):1931-6.
20. Garba ZN, Abdul Rahim A. Evaluation of optimal activated carbon from an agricultural waste for the removal of para-chlorophenol and 2,4-dichlorophenol. *Process Saf Environ Prot*. 2016;102:54-63. doi: [10.1016/j.psep.2016.02.006](https://doi.org/10.1016/j.psep.2016.02.006).
21. García-Araya JF, Beltrán FJ, Álvarez P, Masa FJ. Activated carbon adsorption of some phenolic compounds present in agroindustrial wastewater. *Adsorption*. 2003;9(2):107-15. doi: [10.1023/a:1024228708675](https://doi.org/10.1023/a:1024228708675).
22. Garba ZN, Shikin FB, Abdul Rahim A. Valuation of activated carbon from waste tea for the removal of a basic dye from aqueous solution. *J Chem Eng Chem Res*. 2015;2(5):623-33.
23. Liu X, Wu Y, Ye H, Chen J, Xiao W, Zhou W, Garba ZN, Lawan I, Wang L, Yuan Z. Modification of sugar-based carbon using lanthanum and cobalt bimetal species for effective adsorption of methyl orange. *Environ. Technol. Innov* 2021;23:101769
24. Xiao W, Jiang X, Liu X, Zhou W, Garba ZN, Lawan I, et al. Adsorption of organic dyes from wastewater by metal-doped porous carbon materials. *J Clean Prod*. 2021;284:124773. doi: [10.1016/j.jclepro.2020.124773](https://doi.org/10.1016/j.jclepro.2020.124773).
25. Abdul Rahim A, Garba ZN. Optimization of preparation conditions for activated carbon from *Prosopis africana* seed hulls using response surface methodology. *Desalin Water Treat*. 2016;57(38):17985-94. doi: [10.1080/19443994.2015.1086695](https://doi.org/10.1080/19443994.2015.1086695).
26. Garba ZN, Abdul Rahim A. Process optimization of K₂C₂O₄-activated carbon from *Prosopis africana* seed hulls using response surface methodology. *J Anal Appl Pyrolysis*. 2014;107:306-12. doi: [10.1016/j.jaap.2014.03.016](https://doi.org/10.1016/j.jaap.2014.03.016).
27. Garba ZN, Abdul Rahim A. Potentials of *Prosopis africana* Seed Hulls (PASH) as Precursor for Activated Carbon Preparation Using Sodium Acetate as Activating Agent: Optimization Using Response Surface Methodology. In: *Int Conf Chem Environ Sci Res*; 2014; Penang, Malaysia.
28. Tan IAW, Ahmad AL, Hameed BH. Preparation of activated carbon from coconut husk: optimization study on removal of 2,4,6-trichlorophenol using response surface methodology. *J Hazard Mater*. 2008;153(1-2):709-17. doi: [10.1016/j.jhazmat.2007.09.014](https://doi.org/10.1016/j.jhazmat.2007.09.014).
29. Garba ZN, Abdul Rahim A, Hamza SA. Potential of *Borassus aethiopum* shells as precursor for activated carbon preparation by physico-chemical activation; optimization, equilibrium and kinetic studies. *J Environ Chem Eng*. 2014;2(3):1423-33. doi: [10.1016/j.jece.2014.07.010](https://doi.org/10.1016/j.jece.2014.07.010).
30. Hamad BK, Noor AM, Afida AR, Mohd Asri MN. High removal of 4-chloroguaiacol by high surface area of oil palm shell-activated carbon activated with NaOH from aqueous solution. *Desalination*. 2010;257(1-3):1-7. doi: [10.1016/j.desal.2010.03.007](https://doi.org/10.1016/j.desal.2010.03.007).
31. Hameed BH, Tan IAW, Ahmad AL. Adsorption isotherm, kinetic modeling and mechanism of 2,4,6-trichlorophenol on coconut husk-based activated carbon. *Chem Eng J*. 2008;144(2):235-44. doi: [10.1016/j.cej.2008.01.028](https://doi.org/10.1016/j.cej.2008.01.028).
32. Hamad BK, Ahmad MN, Abdul Rahim A. Removal of 4-chloro-2-methoxy phenol by adsorption from aqueous solution using oil palm shell carbon activated by K₂CO₃. *J Phys Sci*. 2011;22(1):41-58.
33. Langmuir I. The constitution and fundamental properties of solids and liquids. Part I. Solids. *J Am Chem Soc*. 1916;38(11):2221-95. doi: [10.1021/ja02268a002](https://doi.org/10.1021/ja02268a002).
34. Baccar R, Blázquez P, Bouzid J, Feki M, Attiya H, Sarrà M. Modeling of adsorption isotherms and kinetics of a tannery

- dye onto an activated carbon prepared from an agricultural by-product. *Fuel Process Technol.* 2013;106:408-15. doi: [10.1016/j.fuproc.2012.09.006](https://doi.org/10.1016/j.fuproc.2012.09.006).
35. Sadaf S, Bhatti HN, Nausheen S, Amin M. Removal of Cr(VI) from wastewater using acid-washed zero-valent iron catalyzed by polyoxometalate under acid conditions: Efficacy, reaction mechanism and influencing factors. *J Taiwan Inst Chem Eng.* 2015;47:160-70.
 36. Freundlich HM. Over the adsorption in solution. *J Phys Chem.* 1906;57:385-470.
 37. Temkin MJ, Pyzhev V. Recent modifications to Langmuir isotherms. *Acta Physicochim.* 1940;12:217-22.
 38. Hameed BH, Chin LH, Rengaraj S. Adsorption of 4-chlorophenol onto activated carbon prepared from rattan sawdust. *Desalination.* 2008;225(1-3):185-98. doi: [10.1016/j.desal.2007.04.095](https://doi.org/10.1016/j.desal.2007.04.095).
 39. Ren L, Zhang J, Li Y, Zhang C. Preparation and evaluation of cattail fiber-based activated carbon for 2,4-dichlorophenol and 2,4,6-trichlorophenol removal. *Chem Eng J.* 2011;168(2):553-61. doi: [10.1016/j.cej.2011.01.021](https://doi.org/10.1016/j.cej.2011.01.021).
 40. Wang SL, Tzou YM, Lu YH, Sheng G. Removal of 3-chlorophenol from water using rice-straw-based carbon. *J Hazard Mater.* 2007;147(1-3):313-8. doi: [10.1016/j.jhazmat.2007.01.031](https://doi.org/10.1016/j.jhazmat.2007.01.031).
 41. Lagergren S, Svenska BK. On the theory of so-called adsorption of dissolved substances. *The Royal Swedish Academy of Sciences Document.* 1898;24:1-13.
 42. Wang L, Zhang J, Zhao R, Li C, Li Y, Zhang C. Adsorption of basic dyes on activated carbon prepared from *Polygonum orientale* Linn: equilibrium, kinetic and thermodynamic studies. *Desalination.* 2010;254(1-3):68-74. doi: [10.1016/j.desal.2009.12.012](https://doi.org/10.1016/j.desal.2009.12.012).
 43. Khaled A, Nemr AE, El-Sikaily A, Abdelwahab O. Removal of Direct N Blue-106 from artificial textile dye effluent using activated carbon from orange peel: adsorption isotherm and kinetic studies. *J Hazard Mater.* 2009;165(1-3):100-10. doi: [10.1016/j.jhazmat.2008.09.122](https://doi.org/10.1016/j.jhazmat.2008.09.122).
 44. Slimani R, El Ouahabi I, Abidi F, El Haddad M, Regti A, Laamari MR, et al. Calcined eggshells as a new biosorbent to remove basic dye from aqueous solutions: thermodynamics, kinetics, isotherms and error analysis. *J Taiwan Inst Chem Eng.* 2014;45(4):1578-87. doi: [10.1016/j.jtice.2013.10.009](https://doi.org/10.1016/j.jtice.2013.10.009).
 45. Hameed BH. Equilibrium and kinetics studies of 2,4,6-trichlorophenol adsorption onto activated clay. *Colloids Surf A Physicochem Eng Asp.* 2007;307(1):45-52. doi: [10.1016/j.colsurfa.2007.05.002](https://doi.org/10.1016/j.colsurfa.2007.05.002).
 46. Li Q, Yue QY, Su Y, Gao BY, Sun HJ. Equilibrium, thermodynamics and process design to minimize adsorbent amount for the adsorption of acid dyes onto cationic polymer-loaded bentonite. *Chem Eng J.* 2010;158(3):489-97. doi: [10.1016/j.cej.2010.01.033](https://doi.org/10.1016/j.cej.2010.01.033).
 47. Agarry SE, Owabor CN, Ajani AO. Modified plantain peel as cellulose-based low-cost adsorbent for the removal of 2,6-dichlorophenol from aqueous solution: adsorption isotherms, kinetic modeling, and thermodynamic studies. *Chem Eng Commun.* 2013;200(8):1121-47. doi: [10.1080/00986445.2012.740534](https://doi.org/10.1080/00986445.2012.740534).
 48. Sathishkumar M, Binupriya AR, Kavitha D, Yun SE. Kinetic and isothermal studies on liquid-phase adsorption of 2,4-dichlorophenol by palm pith carbon. *Bioresour Technol.* 2007;98(4):866-73. doi: [10.1016/j.biortech.2006.03.002](https://doi.org/10.1016/j.biortech.2006.03.002).